NONLINEAR RESPONSE OF THIN CYLINDRICAL SHELLS WITH LONGITUDINAL CRACKS AND SUBJECTED TO INTERNAL PRESSURE AND AXIAL COMPRESSION LOADS

James H. Starnes, Jr.* and Cheryl A. Rose†
NASA Langley Research Center
Hampton, Virginia 23681-0001

Abstract

The results of an analytical study of the nonlinear response of a thin unstiffened aluminum cylindrical shell with a longitudinal crack are presented. The shell is analyzed with a nonlinear shell analysis code that maintains the shell in a nonlinear equilibrium state while the crack is grown. The analysis accurately accounts for global and local structural response phenomena. Results are presented for internal pressure, axial compression, and combined internal pressure and axial compression loads. The effects of varying crack length on the nonlinear response of the shell subjected to internal pressure are described. The effects of varying crack length on the prebuckling, buckling and postbuckling responses of the shell subjected to axial compression, and subjected to combined internal pressure and axial compression are also described. The results indicate that the nonlinear interaction between the in-plane stress resultants and the out-of-plane displacements near a crack can significantly affect the structural response of the shell. The results also indicate that crack growth instabilities and shell buckling instabilities can both affect the response of the shell as the crack length is increased.

Introduction

Transport fuselage shell structures are designed to support combinations of internal pressure and mechanical flight loads which can cause the structure to have a geometrically nonlinear structural response. These shell structures are required to have adequate structural integrity so that they do not fail if cracks occur in service. The structural response of a shell structure with a local crack is influenced by the local stress and displacement gradients near the crack and by the internal load distribution in the shell. Local fuselage skin displacements near a crack can be large compared to the fuselage skin thickness, and these displacements can couple with the internal stress resultants in the shell to amplify the magnitudes of the local stresses and displacements near the crack. This nonlinear response must be understood and accurately predicted in order to determine the structural integrity and residual strength of a fuselage structure with damage. Recent studies (e.g., Refs. 1-4) have shown that the stiffness and internal load distributions in a shell will change as a crack grows in the shell, and these changes will affect the local stress and displacement gradients near the crack. These studies show that the structural response and structural integrity of a shell with a crack can be studied analytically by the use of a nonlinear structural analysis procedure that can model crack growth in the shell.

Typical nonlinear analysis results presented in Ref. 3 indicate that different combinations of applied loads can cause different responses for a stiffened shell with a long crack. The magnitudes of the stress-intensity factors associated with a long crack in a stiffened fuselage shell are affected significantly by different combinations of internal pressure and bending loads. The results in Ref. 3 indicate that the magnitude of the crack-opening stress-intensity factor for a shell subjected to internal pressure and an axial tension load is less than the magnitude of the corresponding stress-intensity factor for internal pressure only. The results also indicate that the magnitude of the crack-opening stress-intensity factor for a shell subjected to internal pressure and an axial compression load is greater than the magnitude of the corresponding stress-intensity factor for internal pressure only. The magnitude of this stress-intensity factor for an axial compression load and internal pressure is greater than the corresponding magnitudes of the other two loading conditions because the nonlinear coupling between the axial compression stresses and the out-of-plane displacements near the crack amplifies the magnitudes of the local stresses and displacements.

The magnitudes of the mechanical loads used in the studies described in Refs. 3 and 4 are representative of loads that do not buckle the skin of the fuselage. Fuselage shells are usually designed to allow the fuselage skin to buckle above a specified design load that is less than the design limit load for the shell. During the design of the fuselage, it is assumed that the design limit

*Head, Structural Mechanics Branch. Fellow, AIAA.

†Aerospace Engineer, Structural Mechanics Branch. Member, AIAA.

load can occur anytime during the service life of the aircraft. As a result, a long crack could exist in the fuselage shell after a considerable amount of flight service, and loading conditions could occur that cause the shell with the long crack to buckle. Most nonlinear response and residual strength analyses that have been conducted to date for fuselage shells with long cracks have been limited to an unbuckled fuselage shell response.

The present paper describes the results of a nonlinear analytical study of the effects of internal pressure loading, axial compression loading and combined pressure and axial compression loading on the prebuckling, buckling and postbuckling responses of a typical, thin, unstiffened aluminum cylindrical shell with a longitudinal crack. Predicted prebuckling and initial postbuckling deformation patterns and stress resultant distributions are presented for the different loading conditions and crack lengths. The effect of crack length on the initiation of stable tearing and unstable crack growth is discussed. The nonlinear analysis procedure used in the study is also described.

Shell Model and Analysis Procedure

Shell Model

The geometry of the shell analyzed in this study is described in figure 1a. The shell has a 9.0-inch radius, a 0.040-inch-thick wall, and is 36.0 inches long. A longitudinal crack is located at $\theta = 0^{o}$, at the shell mid-length. The initial crack length ranges from 1.0 to 4.0 inches. The shell is a typical laboratory-scale cylindrical shell, made of 2024-T3 aluminum alloy. The Young's modulus, E, for the aluminum alloy is equal to 10 msi and Poisson's ratio is equal to 0.3. The yield stress for the material is 50 ksi and the ultimate stress is 72 ksi.

The loading conditions considered in the study include internal pressure, axial compression and combined internal pressure and axial compression. The maximum value of the applied internal pressure considered is 143 psi. This is the pressure required to cause the shell with a 1.0-inch-long crack to fail due to internal pressure loading only. Internal pressure values equal to 25 psi and 50 psi are considered for the combined loading case. The magnitudes of the axial compression loads are increased from zero to the maximum axial load that the shell can support with a longitudinal crack.

Nonlinear Analysis Procedure

The nonlinear response of the shells was studied numerically using the STAGS (STructural Analysis of General Shells) nonlinear shell analysis code[5]. STAGS is a finite element code for analyzing general shells and includes the effects of geometric and material nonlinearities in the analysis. The code uses both the modified and full Newton methods for its nonlinear solution algorithms, and accounts for large rotations in a shell by using a co-rotational algorithm at the element level. STAGS has static and transient analysis capabilities that can be used to predict local instabilities and modal interactions that occur due to destabilizing mechanical loads, such as an applied compression or shear load. The Riks pseudo arc-length path following method[6, 7] is used to continue a solution past the limit points of a nonlinear response.

STAGS can perform crack-propagation and residual-strength analyses, and can represent the effects of crack growth on nonlinear shell response. A node-release method and a load-relaxation technique are used to extend the length of a crack while the shell is in a nonlinear equilibrium state.[2] The forces necessary to hold the nodes together along the path of new crack growth are calculated with this method. These forces are relaxed as the crack is extended, and a new equilibrium state is calculated which corresponds to the longer crack. The changes in the stiffness matrix and the internal load distribution that occur during crack growth are accounted for in the analysis, and the nonlinear coupling between internal forces and in-plane and out-of-plane displacement gradients that occurs in a shell are properly represented. Results from STAGS calculations include strain-energy-release rates and stress-intensity factors [2, 8] that can be used to calculate the residual strength of a damaged shell. The crack-tip-opening-angle (CTOA) criterion[9] is used to determine when elastic-plastic stable-tearing crack growth will occur.

Both geometric and material nonlinearities were included in the analysis for the pressure only condition. The White-Besseling plasticity theory was used to represent the material nonlinearities. The finite element model used in the analysis for this load case is shown in figure 1b. Symmetry conditions were applied along the edges $\theta = 0^{o}$ and $\theta = 180^{o}$. Internal pressure was simulated by applying an axial tensile force to the ends of the shell, with multi-point constraints to enforce uniform end displacement, and a uniform lateral pressure applied to the shell wall. Initial cracks of lengths 1.0-4.0 inches were defined in the model. A high level of mesh refinement was required around the crack tip to predict accurately yielding at the crack tip, and the crack extension. The crack extension was computed using the CTOA criterion with a critical angle of 4.9^{o}.

The finite element model used for the axial compression and combined internal pressure and axial compression loading conditions is shown in figure 1c. The mesh is refined around the crack to represent the local stress and displacement gradients associated with the crack, and a slightly courser mesh is used for the rest of the shell to represent the deformation modes associated with the nonlinear response and buckling of the shell. For the combined load case, the axial compression and internal pressure were applied in STAGS using two independent load states. The internal pressure loading was simulated as for the pressure only case and axial compression was applied to the ends of the shell by specify-

ing an axial force, and a uniform end displacement.

The prebuckling response of the shells for these two loading conditions was determined using the nonlinear quasi-static analysis capability in STAGS. The initial, unstable, postbuckling response of the shells was predicted using the nonlinear transient analysis option of the code. The transient analysis was initiated from an unstable equilibrium state just beyond the buckling point, by incrementing the end displacement. The transient analysis was continued until the kinetic energy in the system went to zero. A load relaxation was conducted from the point of zero kinetic energy to establish a stable equilibrium state. The stable postbuckling response of the shells was computed using the standard nonlinear, static analysis option.

Results and Discussion

The results of an analytical study of the nonlinear response of a thin unstiffened aluminum cylindrical shell with a longitudinal crack are presented in this section. Results have been generated for three loading conditions that include: internal pressure only; axial compression only; and combined internal pressure and axial compression loads. Results have been generated for longitudinal cracks at shell mid-length with initial crack lengths of 1.0, 2.0, 3.0 and 4.0 inches. Typical results are presented to illustrate the effects of crack length on shell response for the applied loading conditions studied. The effects of varying crack length on the prebuckling, buckling and postbuckling responses of the shell are discussed.

Internal Pressure Loads

The effects of increasing the internal pressure in the shell on the total crack growth or crack extension is shown in figure 2a for shells with initial crack lengths of 1.0, 2.0, 3.0, and 4.0 inches. These results indicate that the internal pressure can be increased until yielding occurs in the material near the crack tips, and then stable tearing of the shell wall occurs that causes the total crack length to increase. Unstable crack growth or fracture of the shell wall occurs when the slope of the curve in figure 2a becomes zero, which means that a small increase in pressure causes a very large crack extension to occur. The results for an initial crack length of 1.0 inch indicate that stable tearing initiates when the internal pressure is approximately 113 psi and unstable crack growth occurs when the internal pressure is approximately 143 psi. The difference between the internal pressure required to initiate stable tearing and the internal pressure that causes unstable crack growth is approximately 30 psi for the 1.0-inch initial crack length. The results for an initial crack length of 2.0 inches indicate that stable tearing initiates when the internal pressure is approximately 51 psi and unstable crack growth occurs when the internal pressure is approximately 79 psi. The difference between the internal pressure required to initiate stable tearing and the internal pressure that causes unstable crack growth for this initial crack length is 28 psi. The difference between the internal pressure required to initiate stable tearing and the internal pressure that causes unstable crack growth for the 3.0- and 4.0-inch initial crack lengths is approximately 24 psi and 21 psi, respectively. These results indicate that the difference in internal pressure between the initiation of stable tearing and unstable crack growth decreases as the initial crack length increases. The effect of increasing the initial crack length on the internal pressure required to initiate stable tearing of the shell wall and to cause unstable crack growth is shown in figure 2b. The lower curve represents initiation of stable tearing and the upper curve represents unstable crack growth. These results indicate that the initial crack length required to initial stable tearing and unstable crack growth decreases as the internal pressure increases.

Contour plots of the hoop stress resultants in the shell with the 3.0-inch initial crack length are shown on the corresponding deformed shapes of the shell in figure 3. Figure 3a shows the entire finite element model used in the analysis and defines the magnified region shown in figures 3b-d. Results are shown in figure 3b for an internal pressure of 21 psi which is less than the pressure required to initiate stable tearing. The results in figure 3c are for an internal pressure of 44 psi after some stable tearing has occurred. The results in figure 3d are for an internal pressure of 54 psi which causes unstable crack growth to occur. The darker and lighter regions in the figures correspond to higher and lower values of the hoop stress resultant, respectively. The increase in the size of the darker regions indicates the increase in the size of the local region with higher values of the hoop stress resultant. The axial and hoop stress resultants near the crack have high values, and these stress resultants increase in magnitude as the crack length increases until the material yields and stable tearing occurs. The modulus of the material is reduced as the material yields, and the effective stiffness of the shell is reduced locally in the plastic zone. The shell is stable until unstable crack growth occurs.

The results in figure 3 also indicate that large outward radial displacements occur in the neighborhood of the crack because of internal pressure. The response associated with these radial displacements is often referred to as "crack bulging" in the literature. The maximum values of the radial displacements near the crack, when the magnitude of the internal pressure is slightly less than the internal pressure required to initiate stable crack growth, increase as the initial crack length increases. The values of this maximum radial displacement, w_{max}, normalized by the shell thickness, t, are $w_{max}/t = 0.36$, 1.58, 2.29 and 2.69 for the 1.0-, 2.0- 3.0- and 4.0-inch-long cracks, respectively. These displacements are greater than or equal to the shell thickness for crack lengths greater than or equal to 2.0 inches, and represent

large displacements in the context of nonlinear thin shell theory.

Axial Compression Loads

A summary of the effects of axial compression loads on the load-shortening results of shells with initial crack lengths of 1.0, 2.0, 3.0 and 4.0 inches is shown in figure 4a. The applied load, P, and the resulting end-shortening displacement, u, in figure 4a are normalized by the linear bifurcation buckling load, P_{cr}, and the corresponding end-shortening displacement, u_{cr}, for a shell without a crack. These results were obtained by increasing the axial compression load until the initial buckling load was determined using the nonlinear static analysis capability in STAGS. The effect of increasing the initial crack length on the initial buckling load of the shell is shown in figure 4b. The response of the shell is unstable for loads greater than or equal to the buckling load and, as a result, the axial load decreases after initial buckling occurs. The initial postbuckling response is determined by using the transient analysis capability in STAGS. The transient analysis is continued until the kinetic energy in the system is equal to zero. A time history of the change in the kinetic energy for a typical analysis is shown in figure 5. Once a stable equilibrium state is determined from the transient analysis, the nonlinear static analysis is resumed until another local buckling mode or the general or overall instability mode occurs. The results shown in figure 4a indicate that the magnitude of the initial buckling loads for the shell deceases as the initial crack length increases. The values of the normalized initial buckling loads are P/P_{cr} = 0.88, 0.59, 0.49 and 0.43 for the 1.0-, 2.0- 3.0- and 4.0-inch-long cracks, respectively. The axial compression loads for the stable postbuckling equilibrium states are much lower in value than the initial buckling loads.

The maximum values of the radial displacements near the crack, for axial compression loads that are slightly less than the initial buckling load, increase as the initial crack length increases. The value of this maximum radial displacement, w_{max}, normalized by the shell thickness, t, is w_{max}/t = 0.2, 1.0, 1.7 and 2.4 for the 1.0-, 2.0- 3.0- and 4.0-inch-long cracks, respectively. These prebuckling displacements are greater than or equal to the shell thickness for crack lengths greater than or equal to 2.0 inches, and represent large displacements in the context of nonlinear thin shell theory.

The postbuckling deformation pattern for the cylinder with a 2.0-inch-long crack is shown in figure 6. The hoop and axial stress resultant distributions near the crack are shown on the right of the figure. The darker regions on the figures represent higher values of the stress resultants and the lighter colors represent lower values of the stress resultants. These results show that the crack has a relatively small, but noticeable, effect on the displacement pattern and stress resultants. For the longer 3.0- and 4.0-inch-long cracks, the radial displacements near the crack are large relative to the shell thickness, and the initial buckling of the shell is a local buckling mode that is followed by a stable local postbuckling response before the shell buckles into its general instability mode. A typical example of the prebuckling radial displacement pattern for the 3.0-inch-long crack is shown in figure 7a. The hoop and axial stress resultant distributions near the crack are shown on the right of the figure. The darker regions on the figure represent higher values of the stress resultants and the lighter regions represent lower values of the stress resultants. These results indicate that the crack has a significant and noticeable effect on the prebuckling displacement pattern and stress resultants. The stable postbuckling deformation shape is shown in figure 7b. The hoop and axial stress resultants near the crack are shown on the right of the figure. The deformation pattern in figure 7b indicates that the shell deforms into a local longitudinal stiffener-like pattern that apparently stiffens the skin near the crack enough to stabilize the shell and increase the amount of axial compression load that can be supported by the shell after initial local buckling occurs.

The results of the analysis indicate that the stress-intensity factors associated with the crack are affected by the load level and the shell equilibrium state. Typical results for the 4.0-in.-long initial crack length indicate that the stress-intensity factors K_I and k_I, which correspond to in-plane crack-opening mode and the crack-bending mode, respectively, are small in value for axial compression loads up to approximately 75% of the initial buckling load. The stress-intensity factor K_I begins to increase from a negligibly small value for the axial compression load that corresponds to u/u_{cr} = 0.30 to a value of 21.0 ksi$\sqrt{in}$ for an applied load that is slightly less than the initial buckling load. This stress-intensity factor then decreases to a value of 11.5 ksi$\sqrt{in}$ at the initial buckling load that corresponds to u/u_{cr} = 0.44. This stress-intensity factor then increases up to a value of 30.5 ksi$\sqrt{in}$ in the postbuckling load range for an applied load that corresponds to u/u_{cr} = 0.62. The stress-intensity factor k_I is very small up to initial buckling and then rapidly increases to a value of 105.4 ksi$\sqrt{in}$ when initial buckling occurs. This stress-intensity factor further increases up to a value of 107.4 ksi$\sqrt{in}$ in the postbuckling load range for an applied load that corresponds to u/u_{cr} = 0.62. These results suggest that a significant amount of local bending occurs near the crack tip at buckling and this local bending continues to increase in the postbuckling load range.

Combined Internal Pressure and Axial Compression Loads

A summary of the effects of combined internal pressure and axial compression loads on the buckling loads for shells with initial crack lengths of 1.0, 2.0, 3.0

and 4.0 inches is shown in figure 8 for 25 and 50 psi of internal pressure. These results indicate that the initial buckling load of the shell increases as the internal pressure increases for a given crack length, because of the tensile hoop stress resultants near the crack. The results also indicate that the buckling load decreases as the crack length increases for a given pressure. The values of the normalized initial buckling loads are $P/P_{cr} = 0.98, 0.75, 0.70$ and 0.63 for the 1.0-, 2.0- 3.0- and 4.0-inch-long cracks, respectively, for 25 psi of internal pressure; and are $P/P_{cr} = 1.12, 0.92, 0.83$ and 0.77 for the 1.0-, 2.0- 3.0- and 4.0-inch-long cracks, respectively, for 50 psi of internal pressure.

The maximum values of the radial displacements near the crack for axial compression loads slightly less than the corresponding initial buckling load increase as the crack length increases. The value of this maximum radial displacement, w_{max}, normalized by the shell thickness, t, is $w_{max}/t = 1.0, 2.7,$ and 6.5 for the 1.0-, 2.0- and 4.0-inch-long cracks, respectively, for 25 psi of internal pressure; and are $w_{max}/t = 1.3, 3.6, 5.8$ and 7.9 for the 1.0-, 2.0- 3.0- and 4.0-inch-long cracks, respectively, for 50 psi of internal pressure. The value for w_{max}/t for the 3.0 inch crack and 25 psi internal pressure is not currently available. A typical example of the prebuckling radial displacement pattern for the 4.0-inch-long crack is shown in figure 9 for 50 psi of internal pressure. These results indicate that increasing the internal pressure changes the prebuckling-deformation results significantly compared to the results for axial compression with no internal pressure.

Concluding Remarks

The results of an analytical study of the effects of a longitudinal crack on the nonlinear response of a thin unstiffened aluminum cylindrical shell subjected to internal pressure, axial compression, and combined internal pressure and axial compression loads are presented. The results indicate that the nonlinear interaction between the in-plane stress resultants and the out-of-plane displacements near a crack in a thin shell can significantly affect the structural response of the shell. Large local stress and displacement gradients exist near a crack in the shell for all loading conditions considered in the study. The results indicate that the nonlinear response of the shell depends on the loading condition applied to the shell and the initial crack length. The magnitude of the internal pressure required to initiate stable tearing in a shell subjected to internal pressure decreases as the initial crack length increases. The magnitude of the internal pressure required to cause unstable crack growth in a shell also decreases as the initial crack length increases. The initial buckling load of a shell subjected to axial compression decreases as the initial crack length increases. Initial buckling causes general instability or collapse of the shell for shorter initial crack lengths. Initial buckling is a stable local response mode for longer initial crack lengths. This stable local buckling response is followed by a stable postbuckling response, which is followed by general or overall instability of the shell. The results for combined internal pressure and axial compression indicate that the initial buckling load of the shell increases as the magnitude of the internal pressure increases, but decreases as the initial crack length increases. Increasing the internal pressure tends to increase the initial buckling load of a shell with a crack, but it also increases the local stresses near the crack and decreases the crack length that initiates stable tearing and unstable crack growth in the shell.

References

[1]Riks, E., "Bulging Cracks in Pressurized Fuselages: A Numerical Study," NLR MP 87058 U, NLR National Aerospace Laboratory, The Netherlands, September 1987.

[2]Rankin, C. C., Brogan, F. A., and Riks, E., "Some Computational Tools for the Analysis of Through Cracks in Stiffened Fuselage Shells," Computational Mechanics, Springer International, Vol. 13, No. 3, December 1993, pp. 143-156.

[3]Starnes, James H., Jr., Britt, Vicki O., and Rankin, Charles C., "Nonlinear Response of Damaged Stiffened Shells Subjected to Combined Internal Pressure and Mechanical Loads," AIAA Paper 95-1462, April 1995.

[4]Starnes, James H., Jr.; Britt, Vicki O.; Rose, Cheryl A.; and Rankin, Charles, C.: "Nonlinear Response and Residual Strength of Damaged Stiffened Shells Subjected to Combined Loads," AIAA Paper No. 96-1555, April 1995.

[5]Brogan, F. A., Rankin, C. C., and Cabiness, H. D., "STAGS User Manual," Lockheed Palo Alto Research Laboratory, Report LMSC P032594, 1994.

[6]Riks, E., "Some Computational Aspects of the Stability Analysis of Nonlinear Structures," Computational Methods in Applied Mechanics and Engineering, Vol. 47, pp. 219-259, 1984.

[7]Riks, E., "Progress in Collapse Analysis," Journal of Pressure Vessel Technology, Vol. 109, 1987, pp. 27-41.

[8]Riks, E., Brogan, F. A., Rankin, C. C., "Bulging of Cracks in Pressurized Fuselages: A Procedure for Computation," in Analytical and Computational Models of Shells, Noor, A. K., Belytschko, T., and Simo, J. C., Editors, The American Society of Mechanical Engineers, ASME-CED Vol. 3, 1989.

[9]Newman, J. C., Jr., Dawicke, D. S., Sutton, M. A. and Bigelow, C. A., "A Fracture Criterion for Widespread Cracking in Thin-Sheet Aluminum Alloys," Proceedings of the ICAF 17th Symposium, 1993.

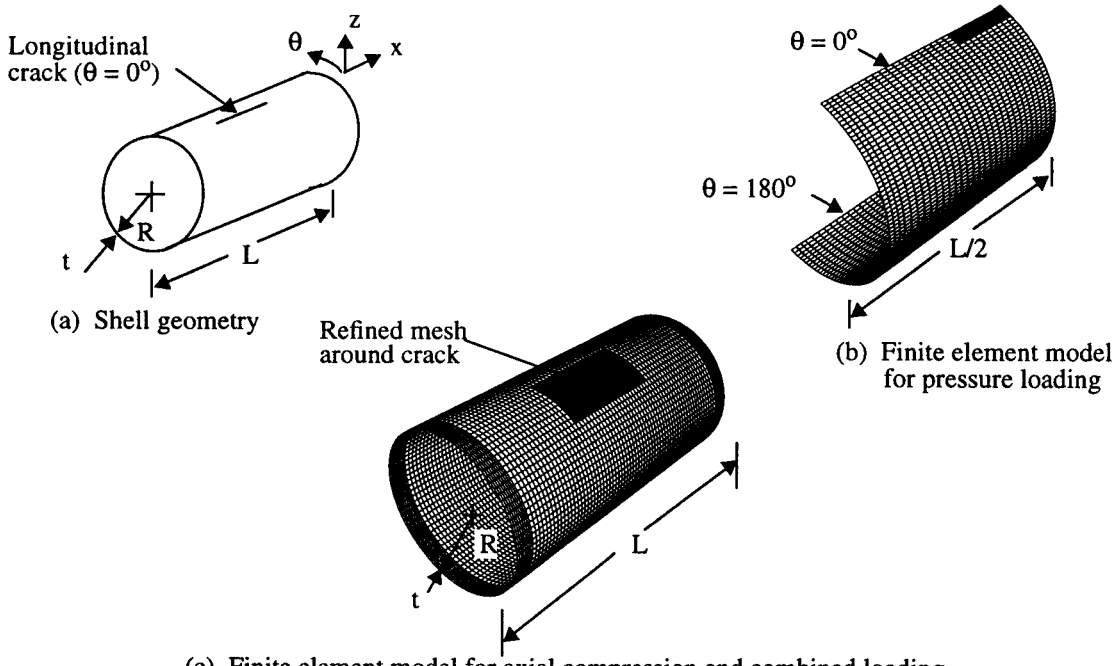

Figure 1. Shell geometry and finite element models.

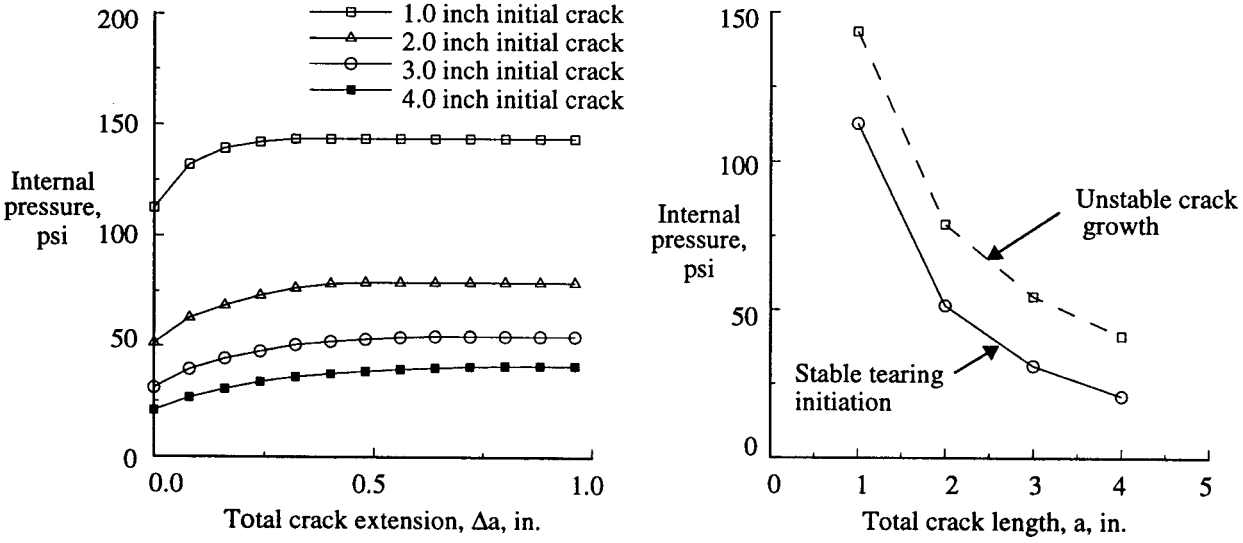

Figure 2. Effect of increasing internal pressure on crack extension, initial stable tearing and unstable crack growth for different initial crack lengths.

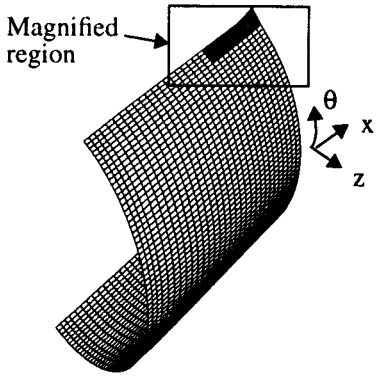

(a) Shell deformations, internal pressure = 44 psi

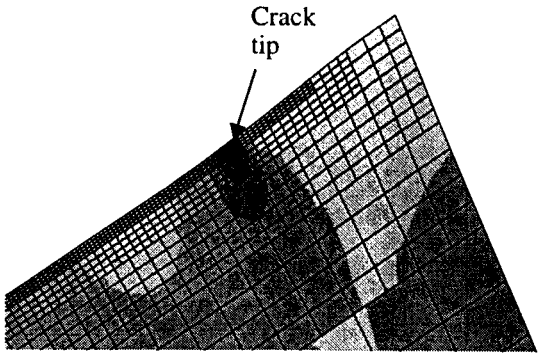

(b) No stable tearing, internal pressure = 21 psi

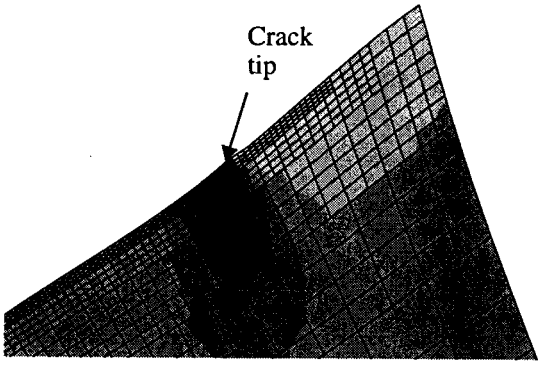

(c) Stable tearing, internal pressure = 44 psi

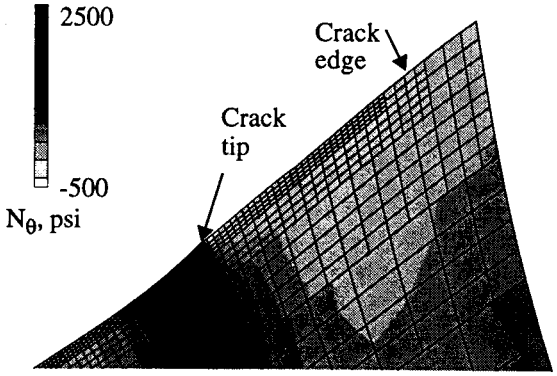

(d) Unstable tearing, internal pressure = 55 psi

Figure 3. Deformed shell and hoop stress resultants for a cylinder with 3.0-inch initial crack length and subjected to internal pressure.

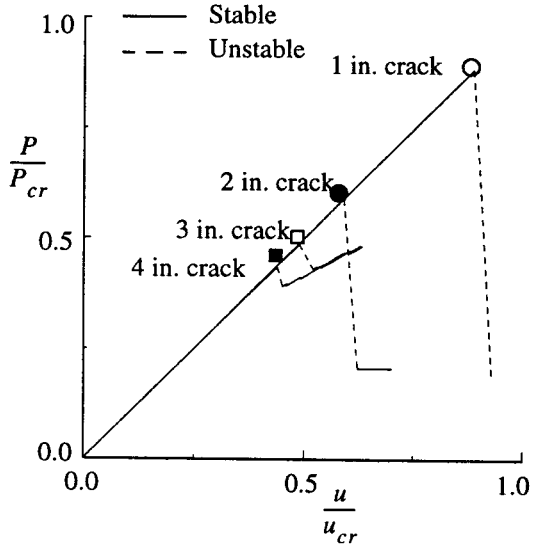

(a) Load-shortening response

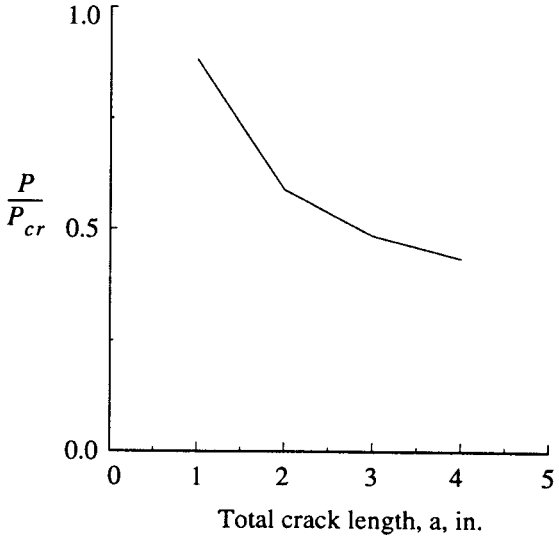

(b) Initial buckling load

Figure 4. Effect of initial crack length on the response of a shell subjected to axial compression.

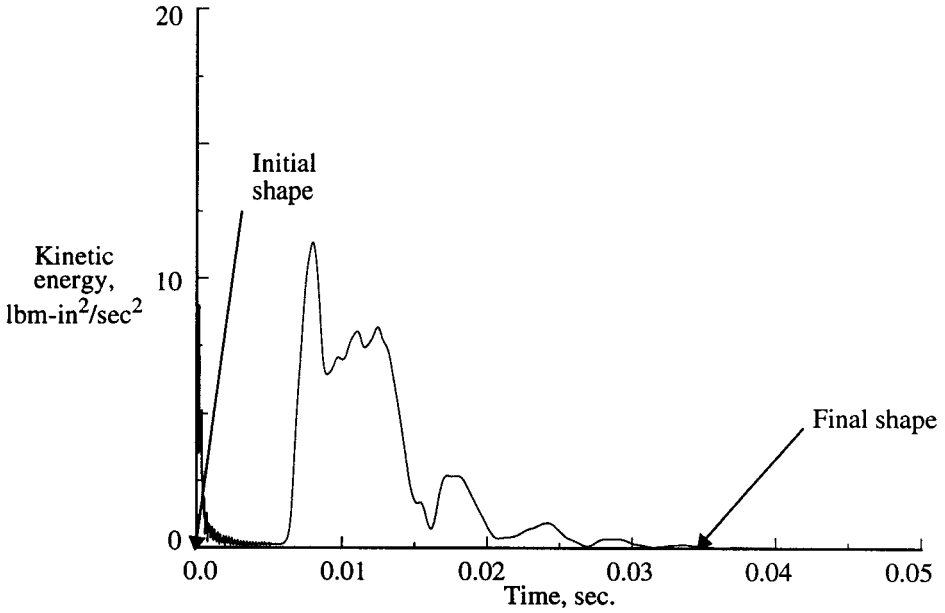

Figure 5. Kinetic energy time history for the unstable buckling reponse of a shell with a 3.0-inch-long crack and subjected to axial compression.

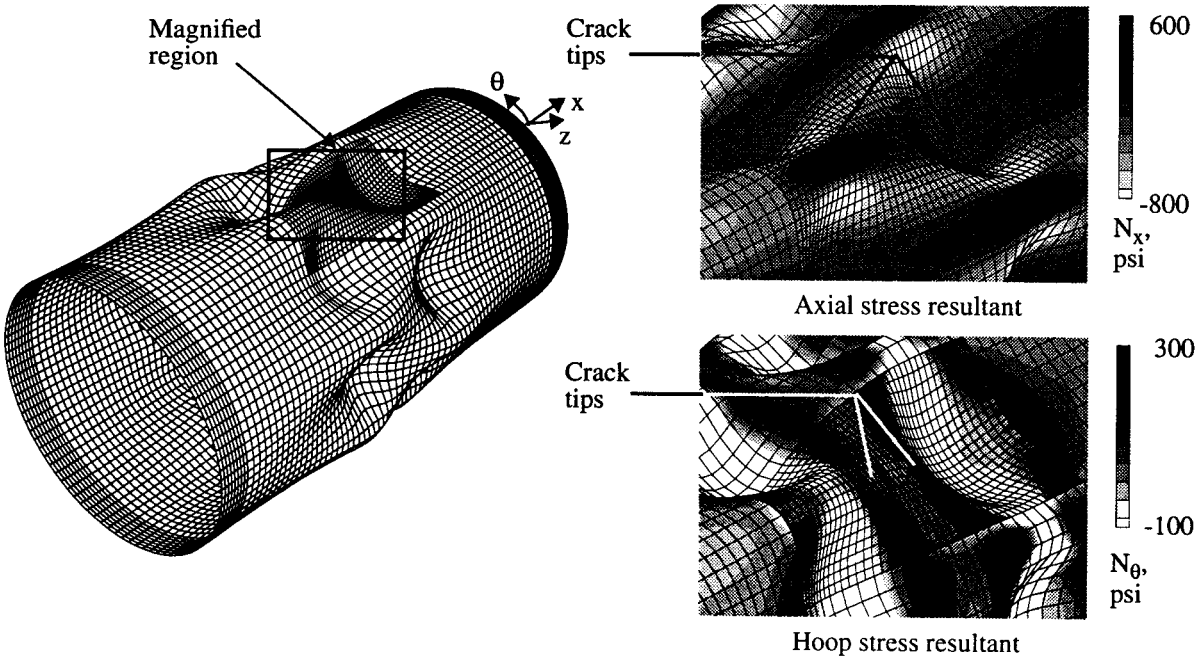

Figure 6. General instability deformation pattern for a shell with a 2.0-inch-long crack and subjected to axial compression.

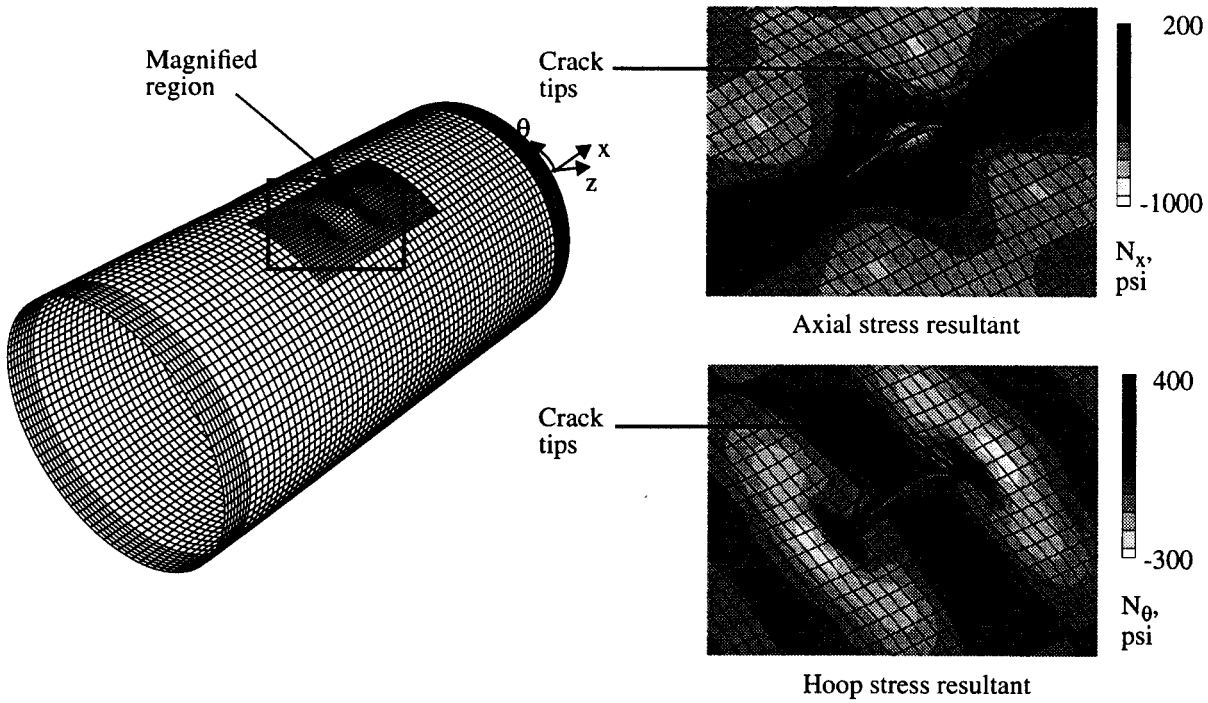

(a) Prebuckling deformation pattern just before initial buckling

Figure 7. Prebuckling and postbuckling deformation patterns for a shell with a 3.0-inch-long crack and subjected to axial compression.

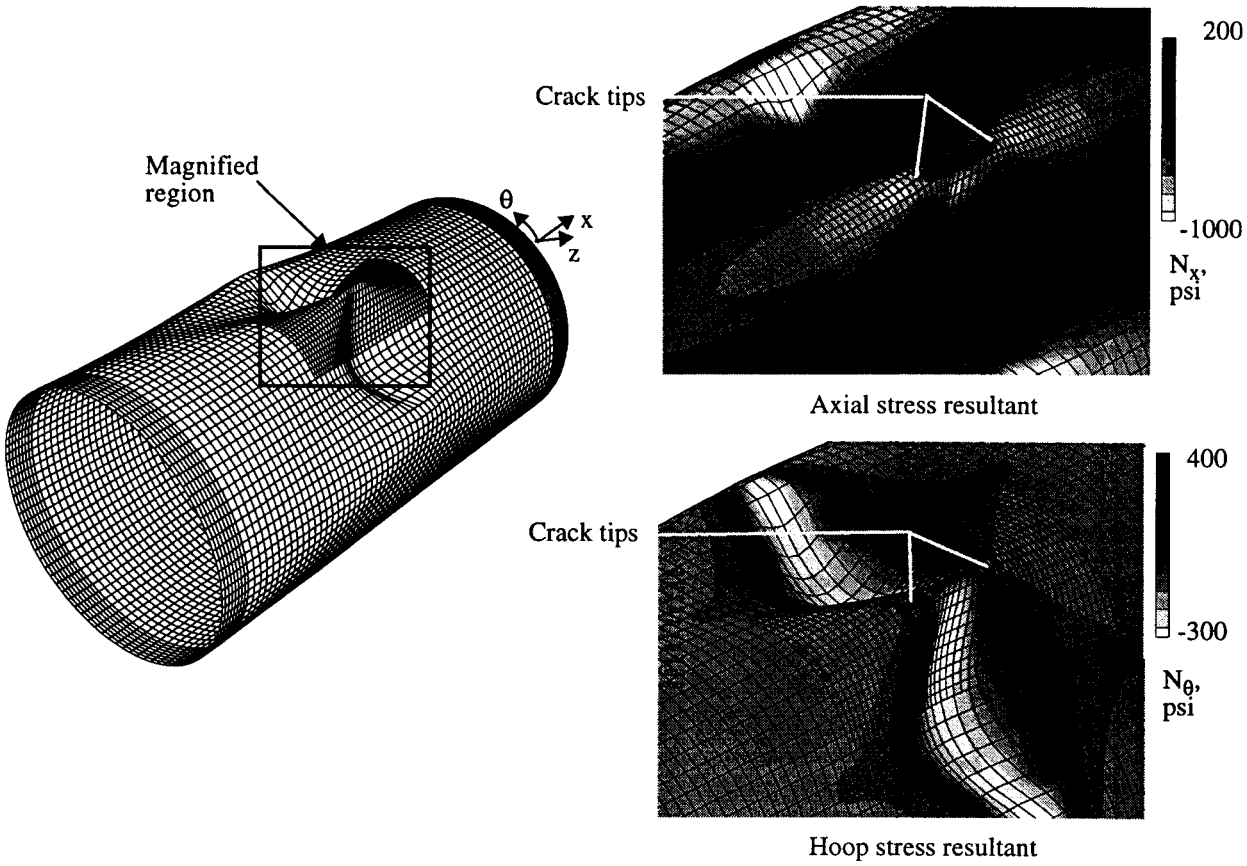

(b) Stable postbuckling deformation pattern

Figure 7. Concluded..

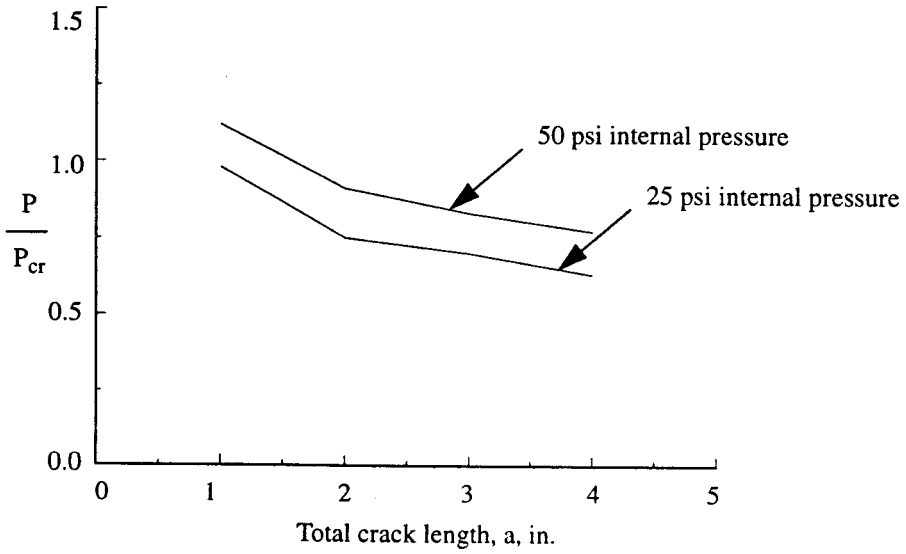

Figure 8. Effect of internal pressure on initial buckling load.

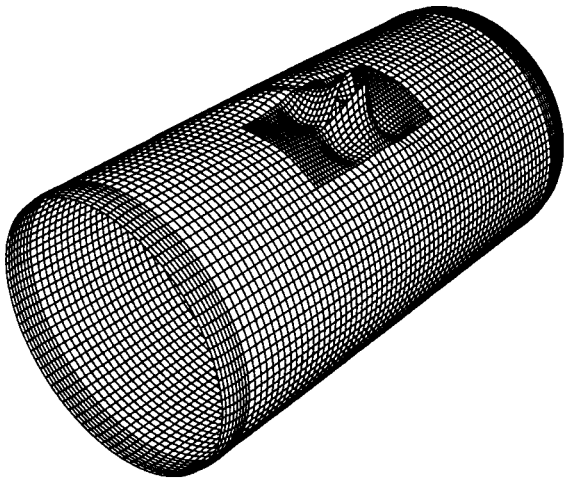

Figure 9. Prebuckling deformation pattern for a shell with a 4.0-inch-long crack and sujbected to axial compression and 50 psi internal pressure.